NOTES AND CORRESPONDENCE

The Effects of Condensational Heating on Midlatitude Transient Waves in Their Mature Stage: Control Experiments with a GFDL General Circulation Model

Y. HAYASHI AND D. G. GOLDER

Geophysical Fluid Dynamics Laboratory/NOAA, Princeton University, Princeton, NJ 08540

2 April 1981 and 24 June 1981

ABSTRACT

The effects of condensational heating on midlatitude transient waves in their mature stage are re-examined by comparing moist and dry GFDL spectral general circulation models, both of which have all ocean surfaces with prescribed zonally uniform temperature. The zonal mean states of both models are fixed in time so as to be identical throughout the time integration.

It is found that the transient eddy kinetic energy is significantly enhanced for all wavenumbers by the effect of latent heat release. This increase is primarily due to an increase in baroclinic conversion from the zonal available potential energy and only partly due to the generation of eddy available potential energy by condensational heating.

1. Introduction

There have been several numerical experiments to study the effects of condensational heating on the development of midlatitude disturbances (Manabe *et al.*, 1970a; Nitta and Ogura, 1972; Gall, 1976c; Ninomiya, 1980) as well as tropical disturbances (Manabe and Smagorinsky, 1967; Manabe *et al.*, 1970b; Hayashi and Golder, 1978).

Manabe *et al.* (1970a) demonstrated, using moist and dry general circulation models, that moist convective adjustment (Manabe *et al.*, 1965) significantly increases energy conversion from eddy available potential energy for high wavenumber (10–20) in the midlatitudes of the model. Without moist convective adjustments, their model exhibited a greater and sharper spectral peak at wavenumber 5, indicating large-scale baroclinic waves. This result seems to be due to the fact that the latitudinal gradient of the mean temperature of the dry model becomes very large in the absence of a meridional transport of latent heat which would reduce the temperature gradient imposed by a sensible heat flux from the surface.

On the other hand, Nitta and Ogura (1972), using a limited domain model with no sensible heat flux from the surface, found a preferential development of intermediate scale (~1000 km ≈ wavenumber 30) cyclones when moist convective adjustment was included. Their model was designed to represent a region with small Richardson number and high humidity. Since the "moist" Richardson number with the effect of condensational heating is of the order of 1, their result was consistent with earlier theoretical studies by Gambo (1970a,b), Tokioka (1970, 1971, 1972, 1973) and Stone (1970, 1971). Their results showed that intermediate-scale cyclones become baroclinically unstable due to non-geostrophic effects if the moist Richardson number is of the order of 1. Recently, Ninomiya (1980) found that the Asian subtropical front is remarkably enhanced by the moist convective adjustment in his forecast model.

The effects of latent heat release on *growing* baroclinic waves was studied by Gall (1976c), using a channel model based on a GFDL general circulation model in which there was no heat flux from the surface. According to his experiment the eddy kinetic energy is enhanced for all wavenumbers (1–30) by an order of magnitude within several days when moist convective adjustment is added to a dry model. However, this result does not necessarily imply that the eddy kinetic energy of a dry model is enhanced by an order of magnitude when the waves are already in a mature stage.

In order to find the climatological effect of condensational heating on transient midlatitude waves, the present paper compares moist and dry general circulation models whose zonally uniform mean states are computationally fixed in time so as to be identical throughout the time integration. It is assumed that this procedure has the same impact on both the models.

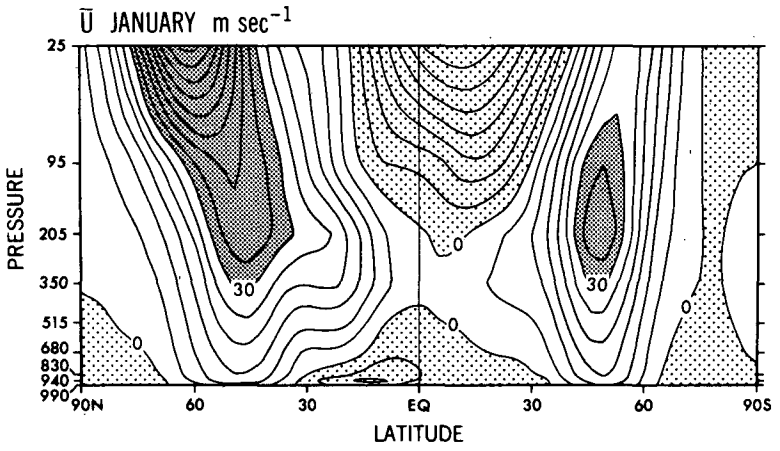

FIG. 1. Latitude–height distribution of the model's zonal wind for January. Contour intervals are 5 m s^{-1}.

The following questions are addressed:

1) Is the kinetic energy of finite-amplitude waves significantly increased by condensational heating in the mature stage?

2) Is the increase primarily due to the generation of eddy available potential energy by condensational heating?

In the next section the models used in the experiments are described, while in Section 3 the results from the moist and dry models are compared. Conclusions and remarks follow in Section 4.

2. Brief description of the models

The present experiments use a model based on a 9-layer, 21-wavenumber (rhomboidal truncation) spectral general circulation model as described in Manabe *et al.* (1979).[1] The biharmonic viscosity coefficient used in the models is given as 0.25×10^{24} cm^4 s^{-1}. The original model's surface is replaced by an all ocean surface with zonally uniform temperatures that were taken from the January zonal mean of ocean and ground temperatures of a 30-wavenumber spectral model with no mountains. This model also supplied the January zonal mean state used in creating the initial conditions for the model's integrations.

Initially, small random disturbances are added to the temperature field and while the integration pro-

[1] Manabe, S., D. G. Hahn, and L. Holloway, Jr., 1979: Climate simulations with GFDL spectral models of the atmosphere: Effect of spectral truncation. *GARP Publ. Series*, No. 22, Vol. 1, 41–94.

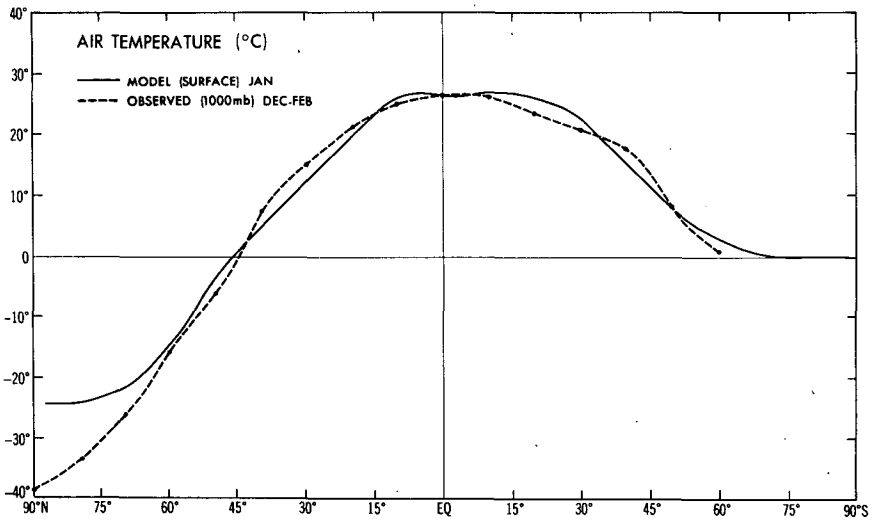

FIG. 2. Latitudinal distribution of zonal mean air temperature (°C). Model (solid curve) at the surface is for the January mean. Observation (dashed curve) at 1000 mb for December–February after Newell *et al.* (1972).

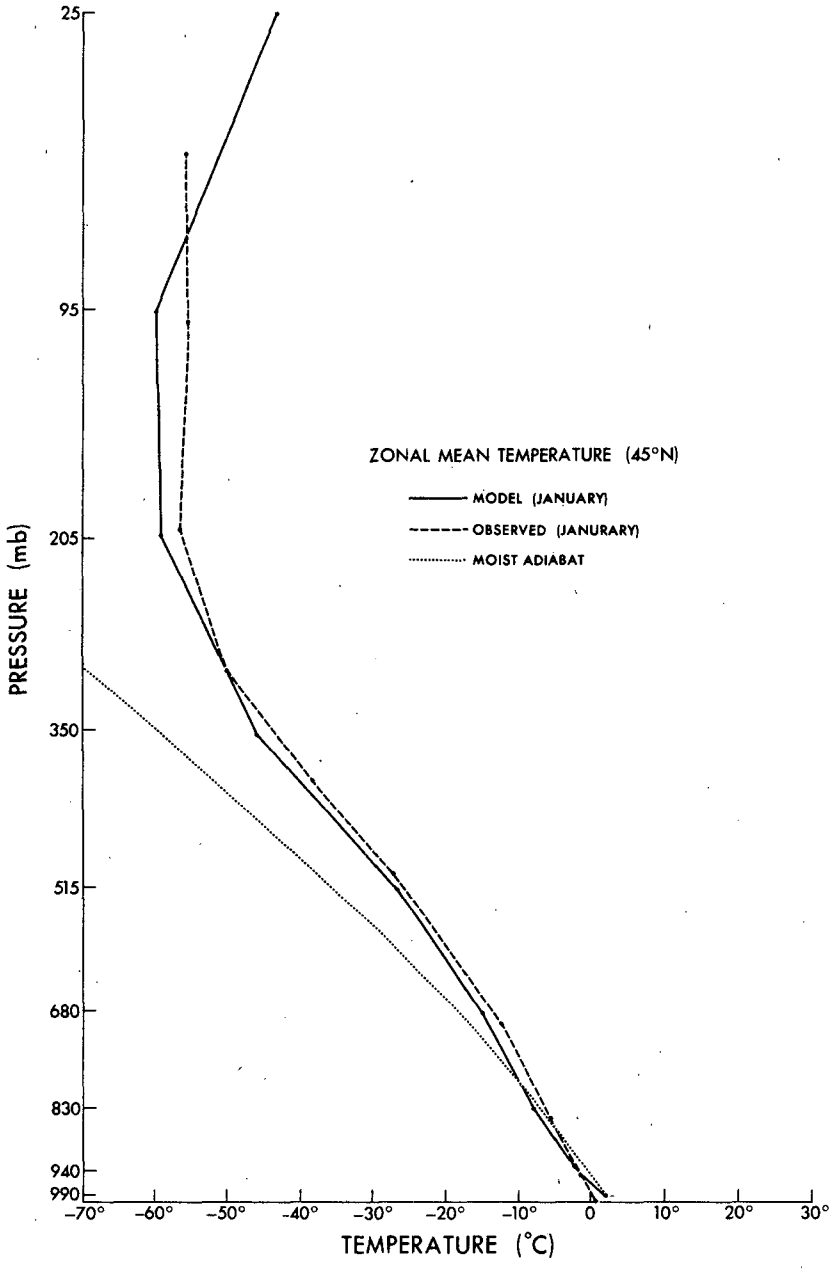

FIG. 3. Vertical distribution at 45°N of zonal mean temperature for January of the model (solid line) and observed (dashed line) taken from Oort and Rasmusson (1971). Dotted line shows a moist adiabat.

ceeds, the zonal mean state is fixed in time by replacing the zonal mean temperature, vorticity and divergence by their initial values. The seasonally varying insolation variables as well as the surface temperature are fixed at January mean values.

In the dry model, moisture has been removed except for the effect of the climatological mean water vapor used in radiation calculations. Also, both models adjust the vertical temperature distribution to the *dry* adiabatic lapse rate, whenever the stratification becomes dry adiabatically unstable. Previous dry GFDL general circulation models adjusted the vertical temperature distribution to the *moist* adiabatic lapse rate in order to keep the mean stratification realistic. In the present dry model this modification is not necessary since the zonal mean temperature is fixed in time. In the moist model, moist convective adjustment occurs whenever the relative humidity is 100% or greater and the computed lapse rate exceeds the moist adiabatic lapse rate.

Fig. 1 shows the latitude–height distribution of the imposed mean zonal wind. Although the strato-

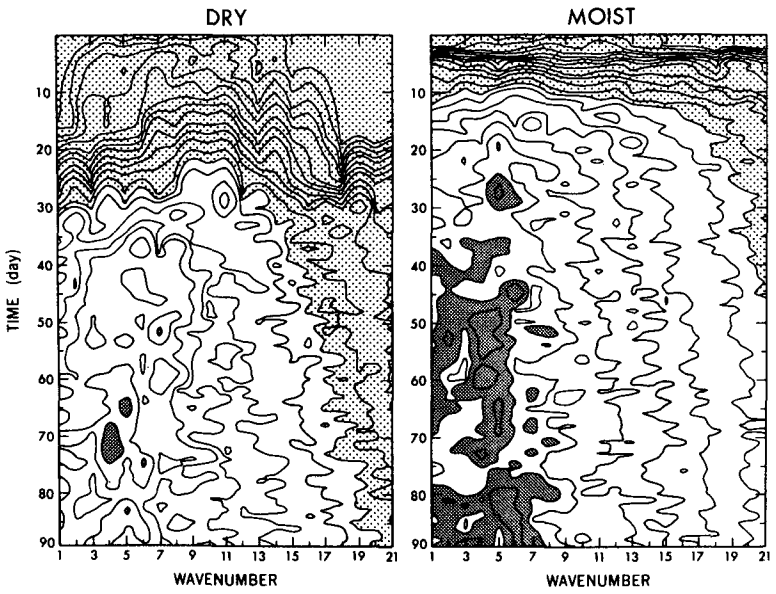

FIG. 4. Wavenumber–time section of kinetic energy integrated vertically over levels 1000–200 mb and latitudes 30–60°N. Dry (left) and moist (right) models. Contour intervals 1, 2, 5×10^{-1}–10^{5} J m^{-2}; dark shade $>1 \times 10^{5}$, light shade $<1 \times 10^{3}$.

spheric westerlies are too strong, it is not likely to have a serious effect on the tropospheric transient waves. Fig. 2 displays the latitudinal distribution of the zonal mean surface temperature as well as the observed 1000 mb temperature for December–January–February. As indicated, there is good agreement between the two. The vertical temperature profile at 45°N of the model and that observed, along with the moist adiabat are shown in Fig. 3. Here, it is indicated that in the lower troposphere the model lapse rate is close to moist adiabatic because of moist convective adjustment, while that observed is less than moist adiabatic.

3. Comparison between moist and dry models

a. Spectral distribution

It is of interest to investigate the effect of condensational heating on the wavenumber spectral distribution of eddy kinetic energy. Fig. 4 shows the wavenumber–time sections of spectral kinetic energy integrated over the tropospheric levels (1000–200 mb) and latitudes 30–60°N. The stratosphere was not included because the zonal mean wind (Fig. 1) is not realistic. It is seen that all the wavenumber components grow faster and attain larger kinetic

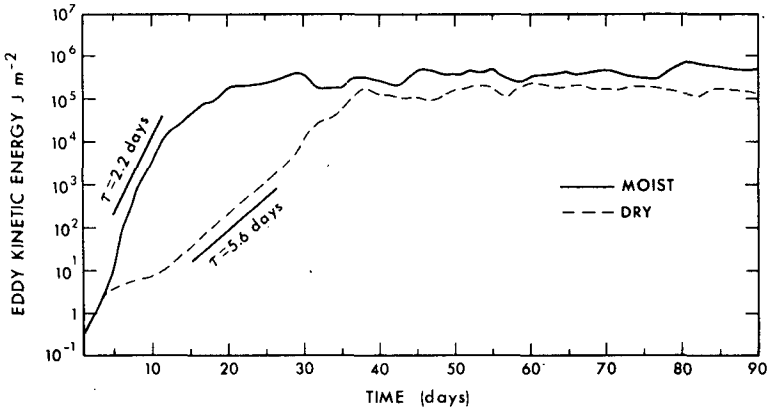

FIG. 5. Time distribution of kinetic energy (wavenumber = 5–8) integrated vertically over 1000–200 mb and averaged over 30–60°N. Moist (solid line) and dry (dashed line) models. The slope of slanted lines indicates e-folding time (τ) of the square root of kinetic energy.

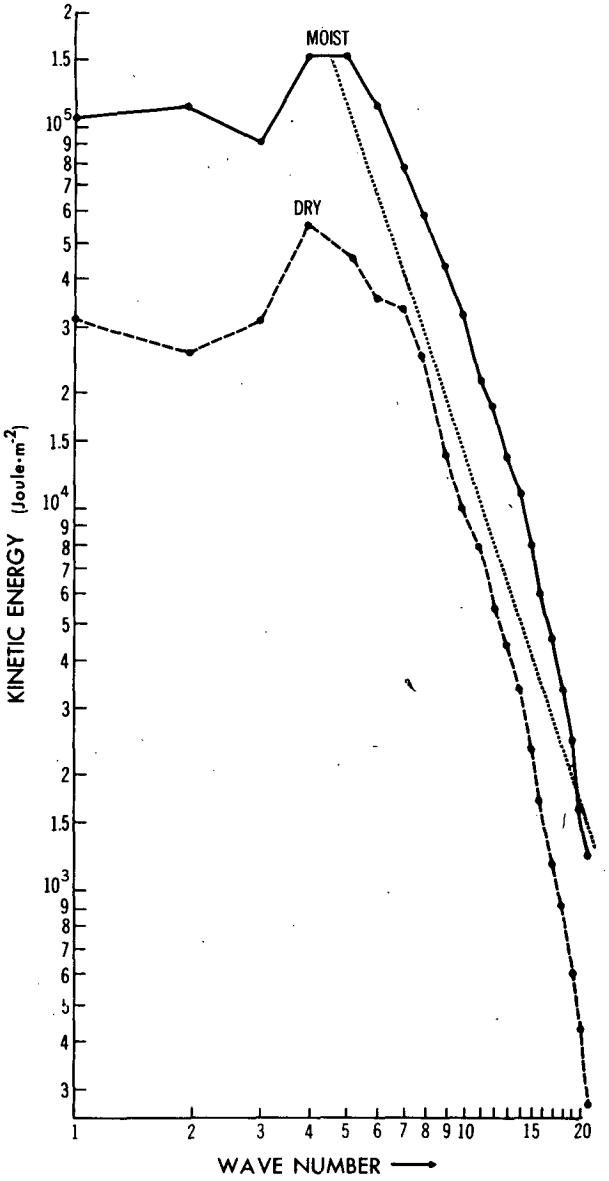

FIG. 6. Wavenumber spectral distribution of kinetic energy integrated over 1000–200 mb and averaged over 30–60°N and days 31–90. Moist (solid line) and dry (dashed line) models. The slanted line indicates −3.0 slope in logarithmic representation.

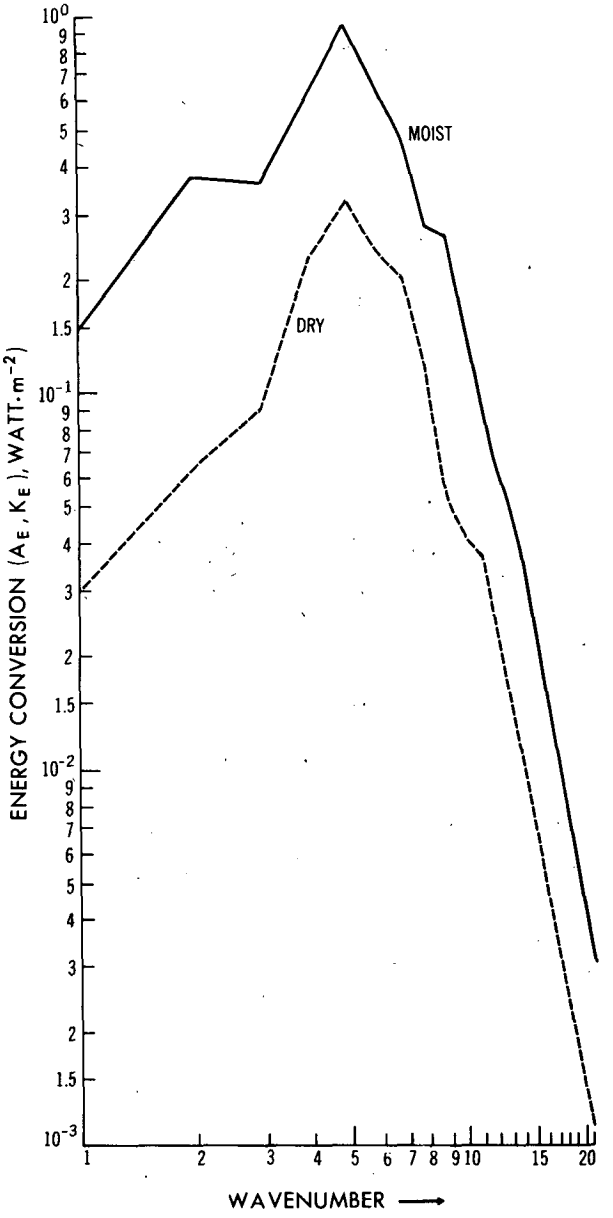

FIG. 7. As in Fig. 6 except for energy conversion (A_E, K_E) from eddy available potential energy to eddy kinetic energy.

energy in the moist model (right) than in the dry model (left).

According to linear models run with realistic basic states (Gall, 1976a; Simmons and Hoskins, 1977; Fredericksen, 1978), the most unstable baroclinic waves are associated with wavenumbers higher than the observed wavenumbers (4–6). Gall (1976b) showed that wavenumber 5 ultimately attains the largest amplitude if a zonal–wave interaction is allowed. The present experiment shows that even when the zonal mean is fixed in time, wavenumbers 4–5 attain the largest eddy kinetic energy. This is probably the result of low wavenumber components being allowed to change with time in the present experiment.

In Fig. 5 the growth of waves with time can be seen in the tropospheric integral of eddy kinetic energy integrated over wavenumbers 5–8. For the first four days of integration there is little difference between the moist and dry waves. This is because the moist model is not initially saturated. At day 15 the dry wave's energy is three orders of magnitude less than that of the moist wave. After day 35 the dry wave has less than half the eddy kinetic energy of the moist wave.

The tropospheric integral of eddy kinetic energy

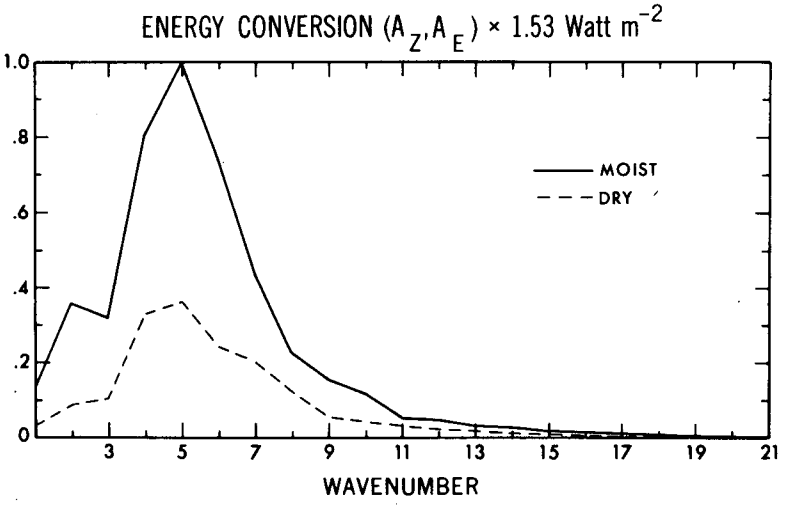

FIG. 8. Wavenumber spectral distribution of energy conversion (A_z, A_E) from zonal available potential energy to eddy available potential energy integrated over 1000–200 mb and averaged over 30–60°N and days 31–90. Moist (solid line) and dry (dashed line) models.

and conversion from eddy available potential energy ($-\overline{\alpha'\omega'}$) in a wavenumber spectral distribution for both the dry and moist waves is presented in Fig. 6 and Fig. 7. The integrals were also averaged over the latitude band 30–60°N and represent the last 60 days of each experiment (days 31–90). Interestingly the relative spectral distribution of the dry wave is not significantly altered in the absence of condensational heating. In particular, the spectral distribution of kinetic energy for wavenumbers greater than 8 is close to the observed minus third power law.

b. Energetics

It also is of interest to investigate the differences in the energetics of the moist and dry waves.

The equation for eddy available potential energy is approximately given by

$$\frac{\partial A_E}{\partial t} = -\nu \frac{\partial T_0}{r\partial\theta}\overline{v'T'} + (\nu/c_p)\overline{T'J'} - \overline{\alpha'\omega'} + \text{nonlinear term}, \quad (3.1)$$

where

$$A_E = \tfrac{1}{2}\nu\overline{T'^2} \quad (3.2)$$

and

$$\nu = \frac{R}{p[\kappa T^H/P - \partial T^H/\partial P]}. \quad (3.3)$$

Here v is the meridional component of the wind, T is the temperature, J is the heating rate per unit mass, α is the specific volume and ω is the vertical pressure velocity. The overbar and prime denote zonal-time

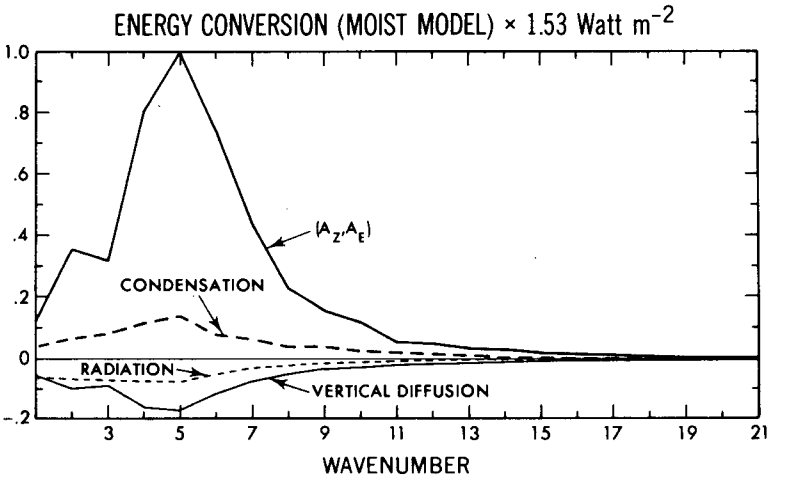

FIG. 9. Wavenumber spectral distribution (moist model) of energy conversion and generation by adiabatic heating integrated over 1000–200 mb and averaged over 30–60°N and days 31–90.

mean and deviation, respectively, and $(\overline{\ })^H$ is the global time average. The explicit expression for the nonlinear term is given by Hayashi (1980), although this term is not estimated in the present paper.

By viewing Fig. 8 it can be seen that the conversion term of zonal to eddy available potential energy is halved in the absence of condensational heating. Fig. 9 shows that the generation of eddy available potential energy by condensational heating is ~10% of the baroclinic conversion and is counterbalanced by radiational effects and the vertical diffusion of temperature. Observationally, condensational heating contributes very little to the energetics of extratropical cyclones (for a review see Smith, 1980).

Thus, energetically, the decrease of eddy kinetic energy in the dry wave is primarily due to the reduction in the conversion from zonal available potential energy and only partly due to the absence of condensational heating.

4. Conclusions and remarks

By comparing moist and dry general circulation models with identical zonal mean states fixed in time, the following conclusions were found:

(i) The transient eddy kinetic energy in the mature stage is significantly increased for all the wavenumbers (1–21) by the effect of condensational heating.

(ii) This enhancement is primarily due to an increase in baroclinic conversion from zonal available potential energy and only partly due to the generation of eddy available potential energy by condensational heating.

The conclusion reached in (i) differs from that of Manabe *et al.* (1970a) who found a larger and sharper spectral peak at wavenumber 5 in their dry model than they found in their moist model. However, their dry model was associated with a larger latitudinal temperature gradient than their moist model, whereas the models used in the present study have identical and fixed temperature gradients. The effect of condensation, or rather the lack of it, may explain why Kida (1977) found very little eddy kinetic energy in his dry general circulation model in which the zonal mean temperature is kept close to that observed by Newtonian cooling.

The conclusion (ii) may be explained, to some extent, by the increase in growth rate due to reduced static stability by the effects of condensation. The model's Richardson number is typically ~20 in the lower troposphere's midlatitudes in the winter hemisphere, while the moist Richardson number defined by the use of the equivalent potential temperature is ~10. This reduction in static stability increases the growth rate of wavenumber 5 by a factor of 2 based on the dispersion relation given by Phillips' (1954) quasi-geostrophic two-layer model. The increase in baroclinic conversion at the low wavenumbers may be due to nonlinear interactions with the higher wavenumbers.

Acknowledgments. The authors wish to express their hearty appreciation to Dr. S. Manabe for his advice and to Dr. J. Smagorinsky for his support of this study. We are also grateful to Drs. C. T. Gordon and R. N. Keshavamurti for their comments. Thanks are extended to P. Tunison for drafting, J. Conner for photographing and J. Kennedy for typing.

REFERENCES

Frederiksen, J. S., 1978: Growth rates and phase speeds of baroclinic waves in multi-level models on a sphere. *J. Atmos. Sci.*, **35**, 1816–1826.

Gall, R. L., 1976a: A comparison of linear baroclinic instability theory with the eddy statistics of a general circulation model. *J. Atmos. Sci.*, **33**, 349–373.

——, 1976b: Structural changes of growing baroclinic waves. *J. Atmos. Sci.*, **33**, 374–390.

——, 1976c: The effects of released latent heat in growing baroclinic waves. *J. Atmos. Sci.*, **33**, 1686–1701.

Gambo, K., 1970a: The characteristic features of medium-scale disturbances in the atmosphere (I). *J. Meteor. Soc. Japan*, **48**, 178–184.

——, 1970b: The characteristic features of medium-scale disturbances in the atmosphere (II). *J. Meteor. Soc. Japan*, **48**, 315–330.

Hayashi, Y., 1980: Estimation of nonlinear energy transfer spectra by the cross-spectral method. *J. Atmos. Sci.*, **37**, 299–307.

——, and D. G. Golder, 1977: Space-time spectral analysis of midlatitude disturbances appearing in a GFDL general circulation model. *J. Atmos. Sci.*, **34**, 237–262.

—— and ——, 1978: The generation of equatorial transient planetary waves: Control experiments with a GFDL general circulation model. *J. Atmos. Sci.*, **35**, 2068–2082.

Kida, H., 1977: A numerical investigation of the atmospheric general circulation and stratospheric–tropospheric mass exchange: I. Long-term integration of a simplified general circulation model. *J. Meteor. Soc. Japan*, **55**, 52–70.

Manabe, S., and J. Smagorinsky, 1967: Simulated climatology of a general circulation model with a hydrologic cycle. *Mon. Wea. Rev.*, **95**, 155–169.

——, —— and R. F. Strickler, 1965: Simulated climatology of a general circulation model with a hydrologic cycle. *Mon. Wea. Rev.*, **93**, 769–798.

——, J. L. Holloway, Jr. and H. M. Stone, 1970b: Tropical circulation in a time integration of a global model of the atmosphere. *J. Atmos. Sci.*, **27**, 580–613.

——, J. Smagorinsky, J. L. Holloway, Jr. and H. M. Stone, 1970a: Simulated climatology of a general circulation model with a hydrologic cycle III. Effects of increased horizontal resolution. *Mon. Wea. Rev.*, **98**, 175–212.

Newell, R. E., J. W. Kidson, D. G. Vincent and G. J. Boer, 1972: *The General Circulation of the Tropical Atmosphere and Interactions with Extratropical Latitudes*. Vol. 1, MIT Press, 258 pp.

Ninomiya, K., 1980: Enhancement of Asian subtropical front due to thermodynamic effect of cumulus convections. *J. Meteor. Soc. Japan*, **58**, 1–15.

Nitta, T., and Y. Ogura, 1972: Numerical simulation of the development of the intermediate-scale cyclone in a moist model atmosphere. *J. Atmos. Sci.*, **29**, 1011–1024.

Oort, A. H., and E. M. Rasmusson, 1971: Atmospheric circulation statistics. NOAA Prof. Pap. 5, U.S. Dept. Commerce, 323 pp.

Phillips, N. A., 1954: Energy transformations and meridional circulations associated with simple baroclinic waves in a two-level, quasi-geostrophic model. *Tellus*, **6**, 273–286.

Simmons, A. J., and B. J. Hoskins, 1977: Baroclinic instability on the sphere: solutions with a more realistic tropopause. *J. Atmos. Sci.*, **34**, 581–588.

Smith, P. J., 1980: The energetics of extratropical cyclones. *Rev. Geophys. Space Phys.*, **18**, 378–386.

Stone, P. H., 1970: On non-geostrophic baroclinic stability: Part II. *J. Atmos. Sci.*, **23**, 721–726.

——, 1971: Baroclinic stability under non-hydrostatic conditions. *J. Fluid Mech.*, **45**, 659–672.

Tokioka, T., 1970: Non-geostrophic and non-hydrostatic instability of a baroclinic fluid. *J. Meteor. Soc. Japan, Ser. II*, **48**, 503–520.

——, 1971: Supplement to non-geostrophic and non-hydrostatic stability of a baroclinic fluid and medium-scale disturbances on the fronts. *J. Meteor. Soc. Japan, Ser. II*, **49**, 129–132.

——, 1972: A numerical experiment of medium-scale disturbances: Dry model. *J. Meteor. Soc. Japan*, **50**, 259–270.

——, 1973: A stability study of medium-scale disturbances with inclusion of convective effects. *J. Meteor. Soc. Japan*, **51**, 1–9.